Editors' Suggestion | Featured in Physics

Time-Resolved Observation of Competing Attractive and Repulsive Short-Range Correlations in Strongly Interacting Fermi Gases

A. Amico,[1,2,§] F. Scazza,[1,2,§] G. Valtolina,[1,2,†] P. E. S. Tavares,[1,2,‡] W. Ketterle,[3] M. Inguscio,[1,2] G. Roati,[1,2] and M. Zaccanti[1,2,*]

[1]*LENS and Dipartimento di Fisica e Astronomia, Università di Firenze, 50019 Sesto Fiorentino, Italy*
[2]*Istituto Nazionale di Ottica del Consiglio Nazionale delle Ricerche (INO-CNR), 50019 Sesto Fiorentino, Italy*
[3]*Department of Physics, MIT-Harvard Center for Ultracold Atoms, and Research Laboratory of Electronics, MIT, Cambridge, Massachusetts 02139, USA*

(Received 26 July 2018; published 19 December 2018)

We exploit a time-resolved pump-probe spectroscopic technique to study the out-of-equilibrium dynamics of an ultracold two-component Fermi gas, selectively quenched to strong repulsion along the upper branch of a broad Feshbach resonance. For critical interactions, we find the rapid growth of short-range anticorrelations between repulsive fermions to initially overcome concurrent pairing processes. At longer evolution times, these two competing mechanisms appear to macroscopically coexist in a short-range correlated state of fermions and pairs, unforeseen thus far. Our work provides fundamental insights into the fate of a repulsive Fermi gas, and offers new perspectives towards the exploration of complex dynamical regimes of fermionic matter.

DOI: 10.1103/PhysRevLett.121.253602

Ultracold quantum gases offer a pristine platform for the realization of minimal Hamiltonians, enabling to investigate the relationship between the macroscopic behavior of a many-body system and the interactions between its constituents. In this context, a two-component atomic Fermi gas with tunable short-range repulsive interactions has attracted a growing interest, being regarded as a paradigmatic framework to address the Stoner model of itinerant ferromagnetism [1,2]. However, in contrast with the widely explored case of attractively interacting Fermi gases [3,4], the nature of the repulsive Fermi gas and its instability towards a ferromagnetic state remain largely debated, both in theory [5–15] and experiments [16–21]. This stems from the fact that genuine short-range repulsion only develops along an excited upper energy branch of the many-body system [8,14], which is unstable against relaxation into the paired many-body ground state [3,4], i.e., the lower branch. As a consequence, it is still questioned whether a repulsive Fermi liquid exists at strong coupling, whether ferromagnetic correlations can develop therein, and how they possibly compete with pairing correlations.

Here, we address these open questions by studying the time-resolved spectral response of a balanced spin mixture of ultracold ^{6}Li atoms. We first employ spin-injection radio-frequency (rf) spectroscopy to precisely locate the upper branch, finding that it remains well defined up to strong couplings. Then, in analogy with ultrafast optical spectroscopy in solid state [22,23], we exploit a pump-probe rf scheme to investigate the out-of-equilibrium dynamics of a strongly repulsive Fermi liquid. A first pump pulse selectively transfers the gas to the upper branch, while a second probe spectroscopy pulse monitors the following evolution [see Fig. 1(a)] with a resolution of few Fermi times τ_F, which sets the minimum collective response time in fermionic many-body systems [24]. By tracking the evolution of the atomic probe spectra center and amplitude, we observe the build-up of atomic anticorrelations in the upper branch and the onset of pairing processes into the lower branch. We extract the initial growth rates for both these mechanisms, developing over timescales of few τ_F. In contrast with theoretical predictions for an instantaneously quenched Fermi gas [11], the rate associated with the build-up of short-range correlations between repulsive quasiparticles is found to be faster than the growth rate of pairing processes, albeit comparable with it. At longer evolution times, we observe an unpredicted slowly evolving regime, where a minority population of unpaired fermions coexists with pairs in a short-range correlated state.

We produce weakly interacting mixtures of about 2×10^5 ^{6}Li atoms in a cylindrically shaped optical dipole trap [20,25] [see Fig. 1(a)], equally populating the two lowest hyperfine atomic states, hereafter denoted as 1 and 2, respectively. Unless otherwise specified, the initial system temperature is $T = 0.12(2)T_F$, where T_F is the Fermi temperature [25]. Our spin-injection spectroscopy protocol for balanced mixtures is analogous to that employed for investigating repulsive Fermi polarons [20]. We typically employ 250 μs-long RF pulses, corresponding to a 0.8π pulse for noninteracting atoms, whose detuning $\delta\nu = \nu - \nu_0$ from the bare $2 \to 3$ transition is scanned. Here, 3 denotes the third-to-lowest ^{6}Li hyperfine state. To adjust the interparticle interaction strength, we exploit a broad Feshbach

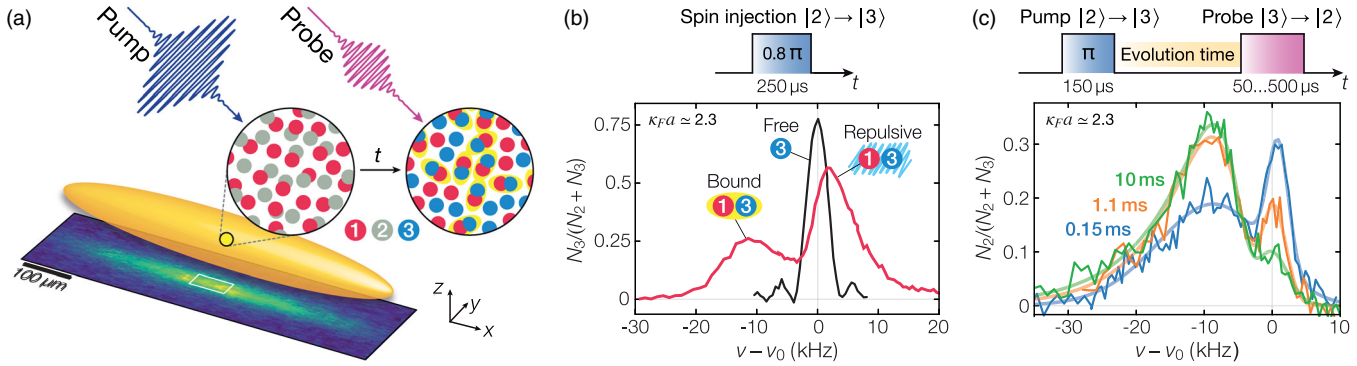

FIG. 1. (a) A pump pulse converts a weakly interacting 1–2 ^{6}Li mixture into a 1–3 strongly repulsive one. After a variable evolution time the gas is probed by a second pulse. The spectroscopic signal is acquired within a central region of the cloud, denoted by a white rectangle in the image. (b) Spin-injection spectrum at $\kappa_F a \simeq 2.3$ (red line). Both the atomic repulsive resonance located at $\Delta_{+0} > 0$ and the pair association spectrum are visible, referenced to the spectrum of a spin-polarized state-2 Fermi gas (black line). The pump pulse remains fully selective up to $\kappa_F a \approx 2.5$, where the atomic and molecular spectral contributions overlap. (c) Probe spectra at $\kappa_F a \simeq 2.3$ for various evolution times (see legend), fitted to a phenomenological model consisting of the sum of Gaussian and Gumbel functions [25]. The spin-injection and pump-probe spectroscopy pulse sequences are also sketched.

resonance between states 1 and 3 located at 690 G [25]. For each magnetic field between 640 G and 680 G, the spectroscopy signal is defined by the fraction of transferred atoms, recorded within the central region of the cloud to reduce the effects of density inhomogeneity [see Fig. 1(a)]. The initial average density $\bar{n}_0$ of state-2 atoms within this region sets the relevant Fermi energy ε_F and wave vector κ_F of the gas [20,25]. The spectral response exhibits two distinct features [see Fig. 1(b)]: an incoherent contribution at $\delta\nu < 0$, related to the binding of two fermions into a 1–3 molecule, clearly detectable only at strong interactions, and a coherent atomic resonance at $\delta\nu > 0$. The latter is associated with the conversion of a weakly interacting mixture into a strongly repulsive Fermi liquid. The center position Δ_{+0} of this atomic peak encodes information about the energy and effective mass of repulsive quasiparticles and their mutual interactions [14,20,37].

We then exploit the knowledge of Δ_{+0} to selectively quench weakly interacting mixtures into the strongly repulsive regime. For each magnetic-field value, an optimized rf pump pulse of about $150\ \mu\text{s} \sim 6\tau_F$, with $\tau_F = \hbar/\varepsilon_F \approx 25\ \mu$s, enables a coherent $2 \to 3$ population transfer to the 1–3 upper branch with high efficiency, exceeding 70% for the strongest couplings investigated here [25]. Immediately after the pump pulse, a 3 μs-long optical blast removes leftover state-2 atoms while negligibly affecting the other spin components. The out-of-equilibrium dynamics of the 1–3 mixture at different interaction strengths is monitored by performing rf spectroscopy on the $3 \to 2$ transition, using a probe pulse applied at variable hold time after the quench. Examples of time-resolved probe spectra are shown in Fig. 1(c). From these, we characterize the evolution of the atomic peak at $\delta\nu > 0$ by extracting its amplitude $A(t)$ and center $\Delta_+(t)$ through Gaussian fits. Owing to their halo character, the weakly bound 1–3 dimers created via inelastic collisions remain optically trapped, and atom-to-molecule conversion does not cause any detectable particle loss. Hence, the decay of $A(t)$ directly reflects the drop of the average fermion density $\bar{n}(t)$ and quantifies the development of pairing processes. Conversely, the peak center $\Delta_+(t)$ provides a measure of the instantaneous (column-integrated) average interaction energy experienced by the surviving state-3 fermions due to the surrounding state-1 atoms and 1–3 pairs. For contact interactions, this is directly linked to the local pair correlator at zero distance $\langle\psi_1^\dagger(\mathbf{r})\psi_3^\dagger(\mathbf{r})\psi_3(\mathbf{r})\psi_1(\mathbf{r})\rangle$, ψ_σ being a state-σ fermion annihilation operator [37]. $\Delta_+(t)$ is also proportional to the contact C [37], which quantifies the number of repulsive fermion pairs at a short distance also in out-of-equilibrium systems [38,39]. Therefore, $\Delta_+(t)$ is sensitive to the development of short-range anticorrelations in the upper branch and to spin-polarized domain formation, both causing a substantial drop of the pair correlator.

Figure 2(a) summarizes the results of our spin-injection spectroscopy studies, shown for $T/T_F \simeq 0.12$ and 0.8. The measured Δ_{+0}, normalized to the Fermi energy ε_F, is displayed as a function of the 1–3 interaction strength, parametrized by $\kappa_F a$, where $a \equiv a_{13}$ is the s-wave scattering length. For both low (orange circles) and high (magenta circles) temperatures, Δ_{+0} is found to progressively increase with increasing repulsion, featuring a trend qualitatively analogous to that observed in the impurity limit of a spin-imbalanced gas (blue squares) [20]. As for this latter case, we attribute the saturation of Δ_{+0} at strong coupling to the mass renormalization of state-2 fermions converted into heavier repulsive quasiparticles [25]. Our data demonstrate the existence of a well-defined repulsive branch for $\kappa_F a \lesssim 2.5$, even in the regime of moderate degeneracy, in spite of an increased atomic spectral width due to enhanced momentum relaxation expected within Fermi liquid theory [25,40].

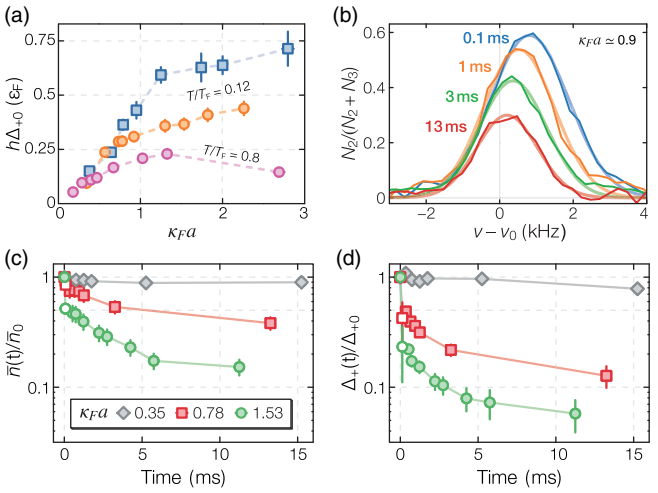

FIG. 2. (a) Interaction shift $h\Delta_{+0}/\varepsilon_F$ as a function of $\kappa_F a$, measured in balanced mixtures at $T/T_F \simeq 0.12$ (orange circles) and $T/T_F \simeq 0.8$ (magenta circles), and in the impurity limit (blue squares) [20]. Vertical error bars combine the standard error of the Gaussian fits to the atomic spectra with the uncertainty in determining ε_F. Horizontal error bars account for the uncertainty in determining κ_F. (b) Examples of atomic probe spectra at $\kappa_F a \simeq 0.9$ for various times after the quench (see legend), together with Gaussian fits. (c) and (d) Evolution of relative fermion density $\bar{n}(t)/\bar{n}_0$ and shift $\Delta_+(t)/\Delta_{+0}$ for different $\kappa_F a$ values (see legend). Colored (white) data points are obtained with a 250 μs-long (50 μs-long) probe pulse. Error bars account for the standard error of the Gaussian fit, and in panel (c) also for the uncertainty in the calibration of $\bar{n}_0$ [25].

Figure 2(b) displays typical time-resolved atomic probe spectra, acquired at $\kappa_F a \simeq 0.9$, together with Gaussian fits used to extract $A(t)$ and $\Delta_+(t)$. Examples of the obtained evolutions at various interaction strengths are shown in Figs. 2(c)–2(d), where both quantities have been normalized to their initial values [25]. In the absence of sizeable particle losses, the trend of $A(t)/A(0)$ is equivalent to that of the relative upper-branch population $\bar{n}(t)/\bar{n}_0$ [see Fig. 2(c)]. While, for weak repulsion, $\bar{n}(t)/\bar{n}_0$ and $\Delta_+(t)/\Delta_{+0}$ show only small and slow variations, their dynamics change qualitatively once the gas is quenched to $\kappa_F a \gtrsim 0.8$. There, both observables exhibit a considerable reduction over submillisecond timescales, progressively faster and more pronounced for increasing $\kappa_F a$. This strongly points to the onset of the pairing instability and to the concurrent growth of anticorrelations between repulsive quasiparticles, possibly arising from a competing ferromagnetic instability [11,21].

We gain quantitative insights into these competing processes by extracting the initial growth rates $\Gamma_{\rm pair}$ and Γ_Δ. To this end, we use linear fits to the evolution at $t \leq 200$ μs of $\bar{n}(t)/\bar{n}_0$ and of $\Delta_+(t)/\Delta_{+0}$, respectively; the linear fits represent the time derivatives of $\bar{n}(t)$ and $\Delta_+(t)$. To increase the time resolution of our spectroscopy protocol, we employ probe pulses as short as 50 μs, yielding for a minimum hold time of 10 μs a highest measurable rate $\Gamma_{\rm max} \sim 0.4\tau_F^{-1}$. When approaching $\Gamma_{\rm max}$, the measured rates should be regarded as lower bounds of the actual ones. For $\kappa_F a \geq 0.8$ both rates increase considerably, with Γ_Δ being larger than $\Gamma_{\rm pair}$ (see Fig. 3). In particular, whereas the former saturates already for $\kappa_F a \sim 1$ near $\Gamma_{\rm max}$, $\Gamma_{\rm pair} \simeq 0.2\tau_F^{-1}$ at $\kappa_F a \simeq 1.6$. In contrast with theoretical expectations [11], we find that atom-atom correlations in the upper branch grow initially faster than the pairing ones. Differently from recent studies of collective spin dynamics [21], the present measurements can identify emerging repulsive short-range correlations, but cannot discern whether these develop within a paramagnetic Fermi liquid [5], or herald instead a ferromagnetic instability. Nonetheless, Γ_Δ reasonably agrees with the predicted growth rate of the most unstable mode of the ferromagnetic instability for a zero-temperature homogeneous Fermi gas [11]. This is expected to establish short-range ferromagnetic correlations at wave vectors of order $\kappa_F/2$ for $\kappa_F a \gtrsim 1$ [11,12,17], promoting the development of ferromagnetic order over a length $\xi \sim (\pi/\kappa_F)(\Gamma_\Delta \tau_F)^{-1/2} \approx 2\pi/\kappa_F \simeq 2.5$ μm, or 1.6 interparticle spacings. Conversely, $\Gamma_{\rm pair}$ is about one order of magnitude lower than the pairing rate obtained in Ref. [11], whereas it fits well to the rate Γ_3 expected for three-body recombination processes [25,41] (see inset of Fig. 3). While this result matches that obtained in the impurity limit [20], our data also agree with previous measurements in balanced mixtures [17]. One reason for the sizable theory-experiment mismatch may be found in the spectral selectivity of the quench protocol employed in this work, and presumably also in Ref. [17]. This starkly contrasts with the instantaneous quench considered in Ref. [11], which projects a noninteracting Fermi gas onto

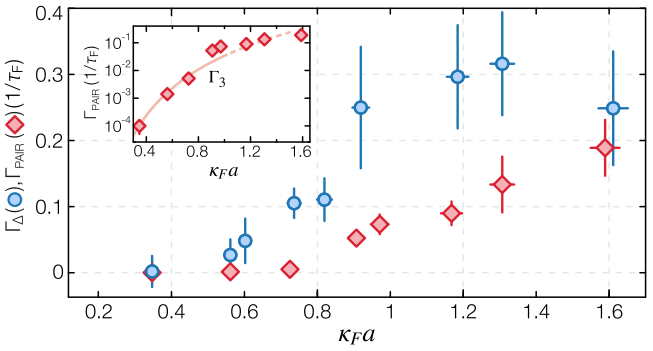

FIG. 3. Growth rates of anticorrelations in the upper branch Γ_Δ (blue circles) and of pairing in the lower branch $\Gamma_{\rm pair}$ (red diamonds), extracted through linear fits to the measured short-time dynamics of $\Delta_+(t)/\Delta_{+0}$ and of $\bar{n}(t)/\bar{n}_0$, respectively. Vertical error bars combine the standard error of the fits with the uncertainty in determining τ_F. Horizontal error bars account for the uncertainty in the determination of κ_F. Inset: $\Gamma_{\rm pair}$ is compared with the predicted three-body recombination rate Γ_3 [25,41].

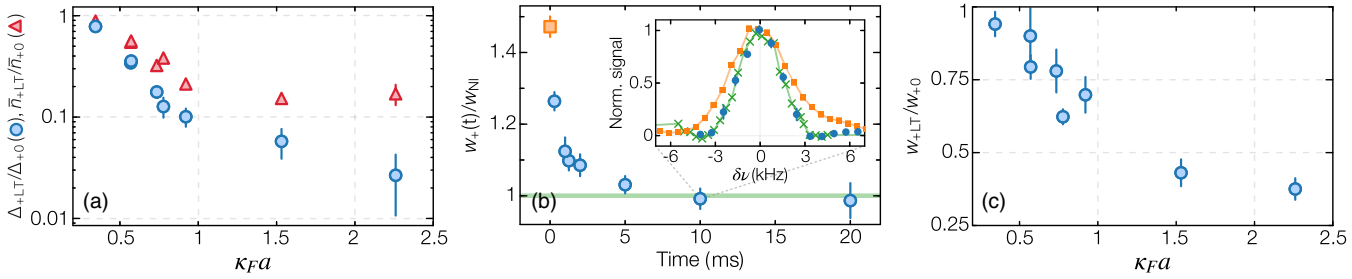

FIG. 4. (a) Relative atomic populations $\bar{n}_{LT}/\bar{n}_0$ (red triangles) and interaction shifts Δ_{+LT}/Δ_{+0} (blue circles), obtained by averaging data points at evolution times $10 \le t \le 30$ ms, as a function of $\kappa_F a$. (b) Evolution of the atomic peak full width at half maximum $w_+(t)$ at $\kappa_F a \simeq 0.9$, normalized to the noninteracting value $w_{\rm NI}$. Inset: atomic probe spectra at $\kappa_F a \simeq 0.9$ recorded at 0 ms (orange squares) and 10 ms (blue circles) after the quench, compared to that of a noninteracting gas (green crosses). The amplitude of each spectrum is normalized to unity and artificially shifted to zero detuning. (c) Spectral width w_{LT} at long times normalized to the $t = 0$ value w_{+0}, as a function of $\kappa_F a$. Vertical error bars in all panels combine the standard error of Gaussian fits to the pump and probe spectra with the standard deviation resulting from averaging several data points.

all available (atomic and molecular) many-body states of the resonant mixture.

Let us now discuss the system evolution at longer times $t \gg \tau_F$. While ferromagnetic correlations in the upper branch could foster domain formation over macroscopic length scales at long evolution times [11,12,15,42], our observations rule out this possibility, which is consistent with Ref. [17]. For $\kappa_F a \gtrsim 1$, despite $\Gamma_{\rm pair} < \Gamma_\Delta$, pairing processes strongly deplete the upper branch population [see Fig. 2(c)], yielding $\bar{n}(t)/\bar{n}_0 < 0.5$ already at $t \sim 1.5$ ms $\sim 50\tau_F$ and a corresponding increase of the molecule density. Although pairing slows down at longer times $t > 100\tau_F$, it likely prevents the growth of anticorrelations between repulsive fermions over distances beyond a few interparticle spacings. The absence of macroscopic spin demixing is supported by real-time measurements of the *in situ* density distributions, which reveal only a maximum twofold increase of local spin-density fluctuations [17,43], attained after 1 ms for $\kappa_F a \approx 1$ [25]. While this moderate enhancement is compatible with the quick formation of microscopic domains, it could also arise from a twofold local temperature increase within a paramagnetic state [25].

Figure 4(a) shows the surviving fermion fraction $\bar{n}_{\rm LT}/\bar{n}_0$ (red triangles) together with the relative interaction shift $\Delta_{+\rm LT}/\Delta_{+0}$ (blue circles), recorded within a long-time (LT) interval $10\ {\rm ms} \le t \le 30$ ms, as a function of $\kappa_F a$. For $\kappa_F a \ge 1$, we find $\bar{n}_{\rm LT}/\bar{n}_0 \approx 0.2$, a value essentially steady over more than 100 ms for $\kappa_F a \simeq 2$. The combined trends of $\bar{n}(t)$ and spin fluctuations would suggest that chemical equilibrium is reached after some transient time within a hotter, incoherent atom-molecule mixture [9,17]. Yet, this interpretation conflicts with other observations. A strong suppression of the interaction shift $\Delta_{+\rm LT}$ is found to persist at long times, with $\Delta_{+\rm LT}/\Delta_{+0} < 0.1$ for $\kappa_F a \ge 1$ [see Fig. 4(a)]. Neglecting atom-pair interactions, such small $\Delta_{+\rm LT}$ values are inconsistent with those measured in a repulsive Fermi liquid at lower density, even when accounting for a twofold temperature increase [25], implying that the surviving atoms remain indeed anticorrelated. On the other hand, atom-pair interactions, which cannot be reasonably ignored for $\bar{n}_{\rm LT}/\bar{n}_0 \lesssim 0.2$, could significantly reduce Δ_+ [25,44] in high-temperature samples, owing to the compensation between atom-pair s-wave repulsion [45] and p-wave attraction [46] at large collision energies. However, the scenario of a hot, uncorrelated atom-molecule mixture is irreconcilable with the observed evolution of the atomic peak width $w_+(t)$ [see, e.g., Fig. 4(b) for $\kappa_F a \simeq 0.9$], which directly reflects the scattering rate of the surviving fermions with the surrounding particles [25,44]. This would be substantially enhanced in a hot incoherent sample since, as for the atom-atom case, the atom-dimer collision rate greatly increases with increasing collision energy [25,46], and would yield $w_+(t)$ much larger than the initial w_{+0}. On the contrary, as directly visible in the probe spectra [see inset of Fig. 4(b)], $w_+(t)$ rapidly decreases below w_{+0}, reaching within experimental uncertainty the Fourier-limited width $w_{\rm NI}$ of the probe pulse, calibrated on a noninteracting sample. Figure 4(c) summarizes the long-time behavior of the spectral width $w_{+\rm LT}$, normalized to the initial value w_{+0} obtained for the pump pulse, as a function of $\kappa_F a$. For $\kappa_F a \ge 1$, $w_{+\rm LT}$ is significantly smaller than w_{+0}, matching the Fourier width of our probe pulse within 10% uncertainty. These observations, together with Rabi oscillation measurements [25], show that the surviving fermions behave as nearly noninteracting particles, although they remain macroscopically overlapped with the paired component at all times. Therefore, the picture of an uncorrelated atom-pair mixture appears too simplistic and qualitatively inconsistent with our data. Rather, our findings suggest that anticorrelated fermions and pairs coexist within a metastable quantum emulsion [47] or glassy state [48,49], where the (two) atomic and molecular many-body wave functions feature a reduced overlap at short distances, possibly as small as a single interparticle spacing [5].

In conclusion, we studied the evolution of a Fermi gas quenched to strong repulsion. We observed the rapid

emergence of short-range anticorrelations between itinerant repulsive fermions, dominating the initial dynamics notwithstanding the concurrent emergence of pairing correlations [11]. These two competing mechanisms appear equally crucial throughout the entire many-body dynamics. Our results clarify previous observations, which were ascribed to a ferromagnetic state of atoms only [16], or to the lack of upper-branch correlations within a rapidly formed atom-molecule incoherent mixture [17]. The observed persistence of strong correlations between repulsive fermions over a long time is also consistent with previous studies of spin dynamics at an artificially created domain wall [21]. In the future, it will be interesting to explore the transport properties of such an exotic atom-molecule mixture, and its robustness in weak optical lattices [42,50] or lower dimensions [51–53]. Our protocols could also provide exciting possibilities to dynamically access elusive regimes of fermionic superfluidity [12,54].

We acknowledge insightful discussions with Tilman Enss, Tin-Lun Ho, Randall Hulet, Pietro Massignan, Dmitry Petrov, Alessio Recati, Tommaso Roscilde, Christian Sanner and Joseph Thywissen. Special thanks to the LENS Quantum Gases group. This work was supported under European Research Council Grants No. 307032 QuFerm2D, and No. 637738 PoLiChroM, Fondazione Cassa di Risparmio di Firenze Project No. 2016.0770 QuSim2D, and the Marie Sklodowska-Curie program (fellowship to F. S.).

*Corresponding author.
zaccanti@lens.unifi.it
†Present address: JILA, University of Colorado, Boulder, Colorado 80309, USA.
‡Present address: Instituto de Física de São Carlos, Universidade de São Paulo, Caixa Postal 369, 13560-970 São Carlos, SP, Brazil.
§A. A. and F. S. contributed equally to this work.

[1] E. Stoner, Philos. Mag. **15**, 1018 (1933).
[2] R. A. Duine and A. H. MacDonald, Phys. Rev. Lett. **95**, 230403 (2005).
[3] *Proceedings of the International School of Physics Enrico Fermi, Course CLXIV*, edited by M. Inguscio, W. Ketterle, and C. Salomon (IOS, Amsterdam, 2007).
[4] *The BCS-BEC Crossover and the Unitary Fermi Gas*, edited by W. Zwerger, Lecture Notes in Physics Vol. 836 (Springer, Berlin, 2012).
[5] H. Zhai, Phys. Rev. A **80**, 051605(R) (2009).
[6] X. Cui and H. Zhai, Phys. Rev. A **81**, 041602(R) (2010).
[7] S. Pilati, G. Bertaina, S. Giorgini, and M. Troyer, Phys. Rev. Lett. **105**, 030405 (2010).
[8] V. B. Shenoy and T.-L. Ho, Phys. Rev. Lett. **107**, 210401 (2011).
[9] S. Zhang and T.-L. Ho, New J. Phys. **13**, 055003 (2011).
[10] S. Chang, M. Randeria, and N. Trivedi, Proc. Natl. Acad. Sci. U.S.A. **108**, 51 (2011).
[11] D. Pekker, M. Babadi, R. Sensarma, N. Zinner, L. Pollet, M. W. Zwierlein, and E. Demler, Phys. Rev. Lett. **106**, 050402 (2011).
[12] I. Sodemann, D. A. Pesin, and A. H. MacDonald, Phys. Rev. A **85**, 033628 (2012).
[13] P. Massignan, Z. Yu, and G. M. Bruun, Phys. Rev. Lett. **110**, 230401 (2013).
[14] P. Massignan, M. Zaccanti, and G. M. Bruun, Rep. Prog. Phys. **77**, 034401 (2014).
[15] L. He, X.-J. Liu, X.-G. Huang, and H. Hu, Phys. Rev. A **93**, 063629 (2016).
[16] G. Jo, Y. Lee, J. Choi, C. A. Christensen, T. H. Kim, J. H. Thywissen, D. E. Pritchard, and W. Ketterle, Science **325**, 1521 (2009).
[17] C. Sanner, E. J. Su, W. Huang, A. Keshet, J. Gillen, and W. Ketterle, Phys. Rev. Lett. **108**, 240404 (2012).
[18] C. Kohstall, M. Zaccanti, M. Jag, A. Trenkwalder, P. Massignan, G. M. Bruun, F. Schreck, and R. Grimm, Nature (London) **485**, 615 (2012).
[19] S. Trotzky, S. Beattie, C. Luciuk, S. Smale, A. B. Bardon, T. Enss, E. Taylor, S. Zhang, and J. H. Thywissen, Phys. Rev. Lett. **114**, 015301 (2015).
[20] F. Scazza, G. Valtolina, P. Massignan, A. Recati, A. Amico, A. Burchianti, C. Fort, M. Inguscio, M. Zaccanti, and G. Roati, Phys. Rev. Lett. **118**, 083602 (2017).
[21] G. Valtolina, F. Scazza, A. Amico, A. Burchianti, A. Recati, T. Enss, M. Inguscio, M. Zaccanti, and G. Roati, Nat. Phys. **13**, 704 (2017).
[22] J. Orenstein, Phys. Today **65**, No. 9, 44 (2012).
[23] C. Giannetti, M. Capone, D. Fausti, M. Fabrizio, F. Parmigiani, and D. Mihailovic, Adv. Phys. **65**, 58 (2016).
[24] M. Cetina, M. Jag, R. S. Lous, I. Fristsche, J. T. M. Walraven, R. Grimm, J. Levinsen, M. M. Parish, R. Schmidt, M. Knap, and E. Demler, Science **354**, 96 (2016).
[25] See Supplemental Material at http://link.aps.org/supplemental/10.1103/PhysRevLett.121.253602 for details on experimental protocols, theoretical models, and spin-density fluctuation measurements, which include Refs. [26–36].
[26] A. Burchianti, G. Valtolina, J. A. Seman, E. Pace, M. De Pas, M. Inguscio, M. Zaccanti, and G. Roati, Phys. Rev. A **90**, 043408 (2014).
[27] G. Zürn, T. Lompe, A. N. Wenz, S. Jochim, P. S. Julienne, and J. M. Hutson, Phys. Rev. Lett. **110**, 135301 (2013).
[28] S. Gupta, Z. Hadzibabic, M. W. Zwierlein, C. A. Stan, K. Dieckmann, C. H. Schunck, E. G. M. van Kempen, B. J. Verhaar, and W. Ketterle, Science **300**, 1723 (2003).
[29] C. A. Regal and D. S. Jin, Phys. Rev. Lett. **90**, 230404 (2003).
[30] Y. I. Shin, A. Schirotzek, C. H. Schunck, and W. Ketterle, Phys. Rev. Lett. **101**, 070404 (2008).
[31] S. Pilati and S. Giorgini, Phys. Rev. Lett. **100**, 030401 (2008).
[32] J. Meineke, Fluctuations and correlations in ultracold Fermi gases, Ph.D. thesis, ETH Zurich, 2012.
[33] C. Sanner, E. J. Su, A. Keshet, R. Gommers, Y.-I. Shin, W. Huang, and W. Ketterle, Phys. Rev. Lett. **105**, 040402 (2010).
[34] T. Müller, B. Zimmermann, J. Meineke, J.-P. Brantut, T. Esslinger, and H. Moritz, Phys. Rev. Lett. **105**, 040401 (2010).

[35] C. Sanner, E. J. Su, A. Keshet, W. Huang, J. Gillen, R. Gommers, and W. Ketterle, Phys. Rev. Lett. **106**, 010402 (2011).
[36] J. Meineke, J.-P. Brantut, D. Stadler, T. Müller, H. Moritz, and T. Esslinger, Nat. Phys. **8**, 454 (2012).
[37] M. W. Zwierlein, *Thermodynamics of Strongly Interacting Fermi Gases* in Proceedings of the International School of Physics Enrico Fermi, Course CXCI, edited by M. Inguscio, W. Ketterle, S. Stringari, and G. Roati (IOS, Amsterdam, 2016), pp. 143–220.
[38] A. B. Bardon, S. Beattie, C. Luciuk, W. Cairncross, D. Fine, N. S. Cheng, G. J. A. Edge, E. Taylor, S. Zhang, S. Trotzky, and J. H. Thywissen, Science **344**, 722 (2014).
[39] R. J. Fletcher, R. Lopes, J. Man, N. Navon, R. P. Smith, M. W. Zwierlein, and Z. Hadzibabic, Science **355**, 377 (2017).
[40] M. Cetina, M. Jag, R. S. Lous, J. T. M. Walraven, R. Grimm, R. S. Christensen, and G. M. Bruun, Phys. Rev. Lett. **115**, 135302 (2015).
[41] D. S. Petrov, Phys. Rev. A **67**, 010703(R) (2003).
[42] I. Zintchenko, L. Wang, and M. Troyer, Eur. Phys. J. B **89**, 180 (2016).
[43] A. Recati and S. Stringari, Phys. Rev. Lett. **106**, 080402 (2011).
[44] M. Jag, M. Zaccanti, M. Cetina, R. S. Lous, F. Schreck, R. Grimm, D. S. Petrov, and J. Levinsen, Phys. Rev. Lett. **112**, 075302 (2014).
[45] D. S. Petrov, C. Salomon, and G. V. Shlyapnikov, Phys. Rev. Lett. **93**, 090404 (2004).
[46] J. Levinsen and D. S. Petrov, Eur. Phys. J. D **65**, 67 (2011).
[47] T. Roscilde and J. I. Cirac, Phys. Rev. Lett. **98**, 190402 (2007).
[48] E. Dagotto, J. Burgy, and A. Moreo, Solid State Commun. **126**, 9 (2003).
[49] J. Schmalian and P. G. Wolynes, Phys. Rev. Lett. **85**, 836 (2000).
[50] S. Pilati, I. Zintchenko, and M. Troyer, Phys. Rev. Lett. **112**, 015301 (2014).
[51] G. J. Conduit, Phys. Rev. A **82**, 043604 (2010).
[52] X. Cui and T.-L. Ho, Phys. Rev. A **89**, 023611 (2014).
[53] C. Luciuk, S. Smale, F. Böttcher, H. Sharum, B. A. Olsen, S. Trotzky, T. Enss, and J. H. Thywissen, Phys. Rev. Lett. **118**, 130405 (2017).
[54] K. H. Bennemann and J. B. Ketterson, *Novel Superfluids* (Oxford University Press, Oxford, 2014), Vol. 2.